

THE SOURCE-LENS CLUSTERING EFFECT IN THE CONTEXT OF LENSING TOMOGRAPHY AND ITS SELF-CALIBRATION

YU YU^{1,*}, PENGJIE ZHANG^{2,1,†}, WEIPENG LIN^{1,‡}, AND WEIGUANG CUI^{3,4}
Apj, 803, 46 (2015)

ABSTRACT

Cosmic shear can only be measured where there are galaxies. This source-lens clustering (SLC) effect has two sources, intrinsic source clustering and cosmic magnification (magnification/size bias). Lensing tomography can suppress the former. However, this reduction is limited by the existence of photo- z error and non-zero redshift bin width. Furthermore, the SLC induced by cosmic magnification can not be reduced by lensing tomography. Through N-body simulations, we quantify the impact of SLC on the lensing power spectrum in the context of lensing tomography. We consider both the standard estimator and the pixel-based estimator. We find that none of them can satisfactorily handle both sources of SLC. (1) For the standard estimator, the SLC induced by both sources can bias the lensing power spectrum by $\mathcal{O}(1\%)$ - $\mathcal{O}(10\%)$. Intrinsic source clustering also increases statistical uncertainties in the measured lensing power spectrum. However, the standard estimator suppresses the intrinsic source clustering in cross spectrum. (2) In contrast, the pixel-based estimator suppresses the SLC by cosmic magnification. However, it fails to suppress the SLC by intrinsic source clustering and the measured lensing power spectrum can be biased low by $\mathcal{O}(1\%)$ - $\mathcal{O}(10\%)$. In a word, for typical photo- z error ($\sigma_z/(1+z) = 0.05$) and photo- z bin size ($\Delta z^P = 0.2$), SLC alters the lensing E-mode power spectrum by 1%-10%, at $\ell \sim 10^3$ and $z_s \sim 1$ of particular interest to weak lensing cosmology. Therefore the SLC is a severe systematic for cosmology in Stage-IV lensing surveys. We present useful scaling relations to self-calibrate the SLC effect.

Subject headings: cosmology: large-scale structure of universe, gravitational lensing: weak

1. INTRODUCTION

Weak gravitational lensing — a powerful probe of the dark universe (Bartelmann & Schneider 2001; Refregier 2003; Munshi et al. 2008; Hoekstra & Jain 2008; Bartelmann 2010; LSST Dark Energy Science Collaboration 2012) — still suffers from many systematic errors. Ongoing lensing surveys like the dark energy survey (DES)⁸ and upcoming surveys such as Euclid⁹, LSST¹⁰, and Subaru-HSC¹¹ will achieve 1% level or better statistical precision. This puts stringent requirements on the accuracy of observational measurement and theoretical modelling (Huterer et al. 2006).

There are various known systematic errors $\sim 1\%$ level in weak lensing measurement (e.g. LSST Dark Energy Science Collaboration 2012 and references therein), including point spread func-

tion, photometric redshift errors and galaxy intrinsic alignment. This motivates highly intensive and comprehensive efforts to understand and calibrate these systematic errors (e.g. Jing 2002; Hirata & Seljak 2004; Jain et al. 2006; Heymans et al. 2006a,b; Waerbeke et al. 2006; Ma et al. 2006; Bridle & King 2007; Joachimi & Schneider 2008; Bridle et al. 2009; Okumura & Jing 2009; Okumura et al. 2009; Joachimi & Bridle 2010; Zhang 2010a,b; Zhang et al. 2010; Bernstein & Huterer 2010; Zhang & Komatsu 2011; Troxel & Ishak 2012a,b,c; Chang et al. 2012, 2013; Hamana et al. 2013; Mandelbaum et al. 2014). Meanwhile, there are various sources of systematic errors in theoretical calculation of weak lensing. (1) The standard treatment adopts the Born approximation. Hence two systematic errors, Born correction and lens-lens coupling (Schneider et al. 1998; Dodelson et al. 2005; Dodelson & Zhang 2005; Dodelson et al. 2006; Hilbert et al. 2009; Becker 2013), arise. It also approximates the measured reduced shear $g \equiv \gamma/(1+\kappa)$ as γ (Schneider et al. 1998; Dodelson & Zhang 2005; Dodelson et al. 2006). (2) The standard treatment neglects the baryon effect on the evolution of the matter density distribution. Studies (White 2004; Zhan & Knox 2004; Jing et al. 2006; Rudd et al. 2008; Zentner et al. 2008; van Daalen et al. 2011; Semboloni et al. 2011, 2013; Zentner et al. 2013; van Daalen et al. 2014; Eifler et al. 2014; Harnois-Déraps et al. 2014) show that baryons can affect the weak lensing power spectrum by $\sim 10\%$ at scales of interest ($\ell \sim 10^3$). (3) Accurate non-linear power spectrum prediction relies on simulations. The modeling at small scales $k \gtrsim 1h\text{Mpc}^{-1}$

¹ Key laboratory for research in galaxies and cosmology, Shanghai Astronomical Observatory, Chinese Academy of Science, 80 Nandan Road, Shanghai, China, 200030

² Center for Astronomy and Astrophysics, Department of Physics and Astronomy, Shanghai Jiao Tong University, 955 Jianchuan Road, Shanghai, 200240

³ ICRAR, University of Western Australia, 35 Stirling Highway, Crawley, Western Australia 6009, Australia

⁴ ARC Centre of Excellence for All-Sky Astrophysics (CAASTRO)

* yuyu22@shao.ac.cn

† zhangpj@sjtu.edu.cn

‡ linwp@shao.ac.cn

⁸ Dark Energy Survey, <http://www.darkenergysurvey.org>

⁹ Euclid, <http://sci.esa.int/euclid/>

¹⁰ Large Synoptic Survey Telescope, <http://www.lsst.org>

¹¹ Subaru Hyper Suprime-Cam, <http://www.naoj.org/Projects/HSC>

can have significant influence on multipoles of $\ell \sim 10^3$. Improperly resolved dark matter substructures also hampers the accurate modeling of lensing signal at small scales (Hagan et al. (2005); McDonald et al. (2006)). (4) It also ignores various selection biases such as the source-lens clustering (SLC). This paper aims to quantify SLC in the context of lensing tomography of typical photometric redshift bin size $\Delta z^P = 0.2$.

The SLC effect (Bernardeau 1998; Hamana 2001) arises from the fact that we can only measure cosmic shear where there are (source) galaxies. Any spatial correlation between the distribution of source galaxies and the lens field (source-lens clustering) can lead to bias in sampling the lensing field and hence lead to biased measurement of lensing statistics. There are two known sources causing such spatial correlation. (1) One is the overlapping of source redshift distribution and lens redshift distribution. Such overlapping is inevitable in reality. We need sufficiently wide redshift bin with sufficient amount of source galaxies to suppress shape measurement noise. For source galaxies in real redshift range of $z_1 < z_s < z_2$, lenses distribute in the range $0 < z_L < z_2$. So sources and lenses overlap at (z_1, z_2) . This overlap causes the intrinsic clustering of source galaxies (δ_g) to be correlated with their cosmic shear $\gamma_{1,2}$ and convergence κ , for both tracing the underlying matter distribution. This correlation leads to biased sampling of the lensing field. Photometric redshift errors further broaden the galaxy distribution in redshift, making the situation worse. (2) The other is the magnification bias (Hamana 2001; Romero et al. 2007), size bias (Schmidt et al. 2009) or any other selection effects depending on the lensing field. For brevity we refer it as cosmic magnification. Lensing changes the galaxy flux/size and hence alters the galaxy number density, $\delta_g \rightarrow \delta_g + g\kappa$ at leading order. Here, g is a function of galaxy flux and size and we refer it to magnification prefactor. It ($g\kappa$) is perfectly correlated with the lensing field (κ). So this effect persists even for source redshift distribution of infinitesimal width.

Impacts of SLC on various weak lensing statistics have been investigated. Bernardeau (1998) showed that SLC by the galaxy intrinsic clustering alters lensing skewness and kurtosis at leading order. Hamana (2001) extended the investigation of skewness to a wide variety of redshift distributions and bias parameters. Hamana et al. (2002) studied SLC by the cosmic magnification using semi-analytical approach. They found that lensing magnification can affect the convergence skewness by $\lesssim 3\%$. Schneider et al. (2002) pointed out that intrinsic source clustering can produce B-mode and presented estimation based on analytical approach. Romero et al. (2007) presented a tool coupling N-body simulations to a semi-analytical model of galaxy formation to perform mock weak lensing measurements, and studied the intrinsic source clustering effect on the probability density distribution (PDF), variance, skewness and kurtosis of the convergence. They found that σ_8 can be biased by 2%-5%. Schmidt et al. (2009) worked on the effect of magnification and size bias on the estimation of shear correlation function. They concluded that this lensing bias should be taken seriously. Their work extended the investigation to 2-point correlation function/power spectrum, compared to the previous works (Hamana 2001;

Hamana et al. 2002) on 1-point variance and skewness. Valageas (2014) adopted hierarchical ansatz and semi-analytic model to estimate the bias caused by the intrinsic source clustering on weak lensing 2-point and 3-point estimators.

Further investigations are still required to fully quantify the impact of SLC on weak lensing modelling and weak lensing cosmology. (1) Most existing works do not focus on SLC in the context of lensing tomography with realistic width of source redshift. These works either study SLC for flux-limited source galaxies with wide redshift distribution (e.g. Bernardeau 1998; Hamana 2001; Hamana et al. 2002; Schneider et al. 2002; Romero et al. 2007) or for fixed source redshift (e.g. Schmidt et al. 2009; Valageas 2014). The impact of SLC for more realistic situation should fall somewhere between the two extreme cases. The SLC caused by the intrinsic source clustering increases with the source redshift width, since the cross correlation between the source and lens increases with the source redshift width. So this kind of SLC effect can be reduced by lensing tomography with finite redshift width. Indeed, in the limit of infinitesimal source redshift width, the SLC effect caused by the intrinsic source clustering can be completely eliminated by the standard estimator (Schmidt et al. 2009). However, photo-z errors and finite galaxy number density prohibit the real redshift width to be smaller than ~ 0.2 . A question to address is then whether in this more realistic situation lensing tomography can suppress the SLC effect to a level negligible. (2) Most existing works calculate SLC approximately. Approximations made include Taylor expanding the cosmic shear estimator and approximations in evaluating high order density correlations. An exception is Romero et al. (2007), which analyzed SLC through N-body simulations and hence avoided these uncertainties. But Romero et al. (2007) only considered the pixel-based estimator, only on 1-point statistics (PDF, variance, etc.), and only for flux-limited galaxies. To make the investigation complete, another estimator (the standard estimator) should also be studied. (3) Given clear evidences that SLC can not be neglected for precision lensing cosmology, an immediate task is to calibrate this effect. For this purpose we shall quantify its dependence on the galaxy bias or the magnification prefactor g in this paper. We find useful scaling relations to correct for the SLC effect.

We will then study the SLC effect through N-body simulation, for photo-z bins of width $\Delta z^P = 0.2$. We will consider both sources of SLC, the intrinsic source clustering and the cosmic magnification. Furthermore, we will consider two popular estimators of shear correlation function/power spectrum. (1) The standard estimator. Cosmic shear is decomposed into the tangential and cross component for each galaxy pair. Then it sums over the two products of shear components over all pairs of fixed angular separation and normalizes by the number of pairs to directly obtain the two point statistics of cosmic shear. This standard estimator is widely used in weak lensing surveys. (2) The pixel-based estimator. It constructs shear maps by averaging over all shears measured in each pixel. One then performs the E-B decomposition and measures the 2-point statistics from these maps. This estimator is convenient for map-making, one point statistics such as peak statistics and PDF, or high-

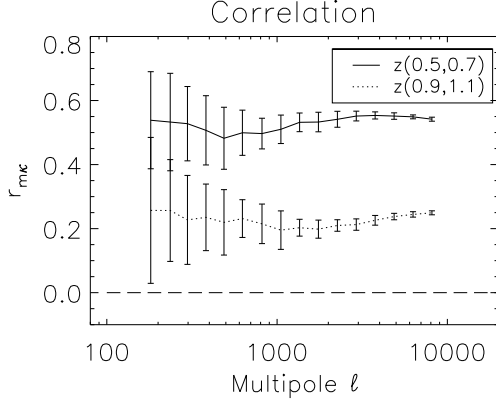


FIG. 1.— Cross correlation coefficient $r_{m\kappa}$ between the source galaxy intrinsic distribution ($b_g = 1$) and the lensing signal. The error bars are the rms dispersion among 20 realizations. In the limit $\sigma_P \rightarrow 0$ and $\Delta z^P \rightarrow 0$, $r_{m\kappa} \rightarrow 0$. But for more realistic cases shown ($\Delta z^P = 0.2$ and $\sigma_P = 0.05(1+z)$), $r_{m\kappa} \sim 0.2-0.6$ at $\ell \sim 1000$, meaning significant spatial correlation between the source galaxies and the lenses. This implies a significant SLC effect, as verified later in the paper. Increasing r with decreasing redshift implies stronger SLC at lower redshift, again verified later in the paper. Notice that this is just one source of SLC. The other source is the cosmic magnification, which is always perfectly correlated with the lensing signal and lensing tomography does not help handle it.

order statistics. The two estimators differ in the order of normalization over the galaxy number density and averaging over galaxy pairs. However, none of them can satisfactorily handle both sources of SLC. Fortunately we find that there exist excellent scaling relations between SLC and observables, which allow for self-calibrating the SLC effect.

Our paper is organized as follows. The SLC effect is described in §2 for both the standard estimator and the pixel-based estimator. The way we estimate the SLC effect through simulation is also described in this section, while the simulation details are attached in the Appendix. The results are presented in §3 & 4 for the standard estimator and the pixel-based estimator, respectively. We discuss and conclude in §5. For busy readers, please refer to Table 1 for figures of major results and corresponding text.

TABLE 1

THE SOURCE-LENS CLUSTERING FOR DIFFERENT ESTIMATORS AND FOR DIFFERENCE SOURCES. BUSY READERS CAN DIRECTLY REFER TO CORRESPONDING FIGURES FOR MAJOR RESULTS AND CORRESPONDING SECTIONS FOR EXPLANATION AND DISCUSSION. OVERALL WE FIND $\mathcal{O}(1)-\mathcal{O}(10)\%$ IMPACT AT TYPICAL SCALE $\ell \sim 10^3$ AND TYPICAL SOURCE REDSHIFT $z_s \sim 1$.

Source-lens clustering (SLC)	The standard estimator	The pixel-based estimator
Intrinsic clustering	§3.1 Fig. 3, 4, 5	§4.1 Fig. 8a, 9, 10
Cosmic magnification	§3.2 Fig. 3, 4, 5, 7	§4.2 Fig. 8b, 9

2. THE SLC EFFECT

Weak lensing cosmology prefers volume weighted lensing measurement. However, in reality we can measure

cosmic shear γ only where there are galaxies. Thus the measured shear field is inevitably weighted by some function of n_g , the number density of observed source galaxies. The galaxy distribution fluctuates spatially, $n_g = \bar{n}_g(1 + \delta^{\text{obs}})$. The limit of no correlation between δ^{obs} and the lensing field (κ and γ) corresponds to randomly sampling the lensing field. This is a fair sampling process and does not bias the measured lensing statistics. Unfortunately, in reality δ^{obs} correlates with the lensing field. So the lensing field is not fairly sampled observationally. Hence this source-lens clustering (SLC) effect biases the lensing measurement.

2.1. The origins of SLC

The observed source galaxy number overdensity δ^{obs} , to leading order, has two components,

$$\delta^{\text{obs}} = \delta_g + g\kappa. \quad (1)$$

Here, δ_g is the intrinsic fluctuation (intrinsic clustering). Throughout the paper we adopt a simple bias model for $\delta_g = b_g \delta_m$ where δ_m is the matter overdensity and b_g is the galaxy bias. $g\kappa$ is that induced by the cosmic magnification. It arises from the thresholds in selecting galaxies, either by flux (magnification bias) or size (size bias).

Since SLC arises from $\delta^{\text{obs}}-\kappa$ (γ) correlation, its strength depends on the cross correlation coefficient $r_{\text{SL}} = C_{\delta^{\text{obs}}\kappa} / \sqrt{C_{\delta^{\text{obs}}\delta^{\text{obs}}} C_{\kappa\kappa}}$ between the two. Here the subscript "SL" denotes "source-lens". $C_{\delta^{\text{obs}}\kappa}$, $C_{\delta^{\text{obs}}\delta^{\text{obs}}}$ and $C_{\kappa\kappa}$ are the cross- and auto-power spectrum between the observed galaxy distribution and lensing convergence. For constant galaxy bias b_g and magnification prefactor g ,

$$r_{\text{SL}}(\ell) = \begin{cases} \frac{C_{m\kappa}(\ell)}{\sqrt{C_{mm}(\ell)C_{\kappa\kappa}(\ell)}} \equiv r_{m\kappa}, & \delta^{\text{obs}} = b_g \delta_m, \\ 1, & \delta^{\text{obs}} = g\kappa. \end{cases} \quad (2)$$

Here $r_{m\kappa}$ is the cross correlation coefficient between the matter distribution and lensing convergence of the source redshift bin.

In Fig. 1, we plot $r_{m\kappa}$ measured through simulation, for two typical photo- z bins, $z^P \in (0.5, 0.7)$ and $(0.9, 1.1)$. We adopt a source distribution

$$n^P(z^P)dz^P = \frac{1}{2} \frac{z^P}{z_0^3} \exp\left(-\frac{z^P}{z_0}\right) dz^P \quad (3)$$

with $z_0 = 0.45$, typical for LSST-like surveys. We assume the photo- z scatter is perfectly known to be in a Gaussian form with photo- z error $\sigma_P = 0.05(1+z)$. In reality lensing survey also suffers from catastrophic errors. The safety line for unbiased dark energy parameters constraints was studied in Hearin et al. (2010). Also several facts prevent us from accurately knowing the scatter function $P(z^P|z)$ (Cunha et al. 2012b,a). However, our assumption captures the main feature of the photo- z error except the catastrophic error. The real galaxy distribution contributing to photo- z bin $(0.5, 0.7)$ and $(0.9, 1.1)$ is shown in Fig. 2. Photo- z errors broaden the redshift distribution and cause substantial overlap between the source and lens distribution. This results in a significant $r_{m\kappa} \sim 0.2-0.6$ at $100 \lesssim \ell \lesssim 10^4$. The correlation strength is stronger towards lower redshift, because of

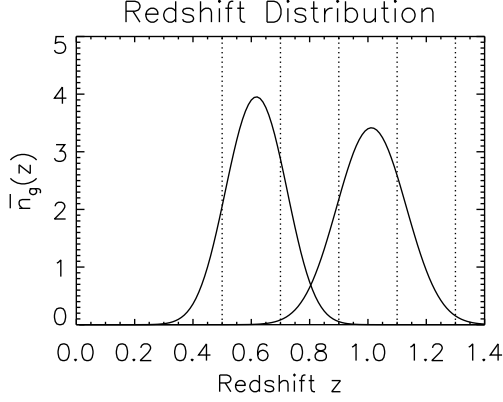


FIG. 2.— The real source galaxy distribution $\bar{n}_g(z)$ of photo- z bins (0.5, 0.7) and (0.9, 1.1) are presented. $\bar{n}_g(z)$ is normalized to $\int \bar{n}_g(z) dz = 1$. Photo- z error broadens the redshift distribution significantly, and hence increases the SLC effect.

the stronger redshift dependence of lensing kernel. This result directly indicates larger SLC effect due to the intrinsic source clustering towards lower redshift¹². The correlation coefficient only shows weak dependence on the scale, indicating that the SLC effect can be important at all scales.

Narrowing the photo- z bin reduces $r_{m\kappa}$. But this reduction is very mild, because the redshift width is $\sim 2\sigma_P \sim 0.2$ even in the limit $\Delta z^P = 0$ for $z_s \sim 1$. Hence even with the aid of photo- z information, SLC induced by the intrinsic source clustering can not be significantly suppressed. We then expect non-negligible SLC even in the context of lensing tomography.

The exact impact of SLC depends on the estimator of these lensing statistics. In this work we investigate two widely used estimators for the 2-point correlation function and power spectrum.

2.2. The standard estimator

The standard estimator (Munshi et al. 2008; Schmidt et al. 2009; Heymans et al. 2012) averages shear products on galaxy pairs in the lensing survey. For each galaxy cosmic shear is decomposed into the tangential shear γ_t and the cross component γ_\times relative to the separation vector to the other galaxy in the pair. Then one calculates the following shear-shear correlation functions:

$$\xi_{\pm}(\theta) = \frac{\sum_{\alpha\beta} [\gamma_{t,\alpha}\gamma_{t,\beta} \pm \gamma_{\times,\alpha}\gamma_{\times,\beta}] w_{\alpha} w_{\beta} \Delta_{\alpha\beta}}{\sum_{\alpha\beta} w_{\alpha} w_{\beta} \Delta_{\alpha\beta}}, \quad (4)$$

where galaxy pairs labeled α, β are separated by angular distance $\vartheta = |\vartheta_{\alpha} - \vartheta_{\beta}|$. $\Delta_{\alpha\beta} = 1$ counts for all the pairs with ϑ falling in the angular bin centered at θ , otherwise $\Delta_{\alpha\beta} = 0$. w_{α} is the weighting for each galaxy depending on some selection factors like the image quality, etc.. For brevity, we only discuss the simplified case $w_{\alpha} = 1$. Ideally (e.g. in the absence of SLC), these correlation functions are connected to the theory through the rela-

¹² We should point out here that the correlation coefficient does not completely determine the strength of SLC. For example, it is invariant to a deterministic galaxy bias. But sources with stronger clustering (larger b_g) has larger SLC effect.

tionship

$$\xi_{+/-}(\theta) = \frac{1}{2\pi} \int_0^{\infty} d\ell \ell J_{0/4}(\ell\theta) C_{\kappa\kappa}(\ell), \quad (5)$$

in which $J_{0/4}$ is the 0th- and 4th-order Bessel function of the first kind. However, as shown above, the SLC effect is implicitly included through the summation over all galaxy pairs.

E-B decomposition is very useful in weak lensing analysis. B-modes are strong evidence for systematic errors, such as the point spread function (Hoekstra 2004), shear calibration errors, galaxy intrinsic alignment, finite volume effect (Kilbinger et al. 2006), and the SLC effect (Schneider et al. 2002). From theoretical aspect, the E/B-mode power spectra are related to the correlation functions as

$$C_{E/B}(\ell) = \pi \int_0^{\infty} d\theta \theta [J_0(\ell\theta) \xi_{+}(\theta) \pm J_4(\ell\theta) \xi_{-}(\theta)]. \quad (6)$$

In simulation implementation, the calculation of E/B-mode power spectrum can be simplified, without calculating ξ_{\pm} . First one measures the shear correlation functions

$$\hat{\xi}_{ij}(\vec{\theta}) = \frac{\langle \int dz \bar{n}_g(z) (1 + \delta^{\text{obs}}(z)) \int dz' \bar{n}_g(z') (1 + \delta^{\text{obs}}(z')) \gamma_i(z) \gamma_j(z') \rangle}{1 + \xi_{\delta^{\text{obs}}}(\theta)}, \quad (7)$$

in which the denominator $(1 + \xi_{\delta^{\text{obs}}}(\theta)) = \langle \int dz \bar{n}_g(z) (1 + \delta^{\text{obs}}(z)) \int dz' \bar{n}_g(z') (1 + \delta^{\text{obs}}(z')) \rangle_{\theta=|\vec{\theta}|}$ is the correlation function of the observed galaxy distribution. It averages over direction of $\vec{\theta}$. But the numerator does not. $i, j = 1, 2$ denote for the shear components defined related to axes. The prime denotes for another line-of-sight with separation $\vec{\theta}$. The integral (summation) is over all galaxies in the bin. This allows us to do a 2D Fourier transform to obtain the corresponding 2D power spectrum $C_{ij}(\vec{\ell}) = \text{FFT}(\hat{\xi}_{ij}(\vec{\theta}))$. We then average over the direction of $\vec{\ell}$ to obtain the E/B-mode power spectrum,

$$\begin{aligned} C_E(\ell) &= \langle C_{11}(\vec{\ell}) \cos^2 2\varphi_{\vec{\ell}} \rangle + \langle C_{22}(\vec{\ell}) \sin^2 2\varphi_{\vec{\ell}} \rangle \\ &\quad + \langle (C_{12}(\vec{\ell}) + C_{21}(\vec{\ell})) \cos 2\varphi_{\vec{\ell}} \sin 2\varphi_{\vec{\ell}} \rangle, \\ C_B(\ell) &= \langle C_{11}(\vec{\ell}) \sin^2 2\varphi_{\vec{\ell}} \rangle + \langle C_{22}(\vec{\ell}) \cos^2 2\varphi_{\vec{\ell}} \rangle \\ &\quad - \langle (C_{12}(\vec{\ell}) + C_{21}(\vec{\ell})) \cos 2\varphi_{\vec{\ell}} \sin 2\varphi_{\vec{\ell}} \rangle. \end{aligned} \quad (8)$$

Here $\varphi_{\vec{\ell}}$ is the angle between the vector $\vec{\ell}$ and the x-axis in 2D Fourier space.

2.3. The pixel-based estimator

For the pixel-based estimator (Schmidt et al. 2009), one directly obtains an averaged cosmic shear γ from all galaxies in each pixel,

$$\hat{\gamma}_i = \frac{\int \bar{n}_g (1 + \delta^{\text{obs}}) \gamma_i dz}{\int \bar{n}_g (1 + \delta^{\text{obs}}) dz}. \quad (9)$$

Then we can construct lensing convergence map through

$$\kappa_E(\vec{\ell}) = \hat{\gamma}_1(\vec{\ell}) \cos 2\varphi_{\vec{\ell}} + \hat{\gamma}_2(\vec{\ell}) \sin 2\varphi_{\vec{\ell}}. \quad (10)$$

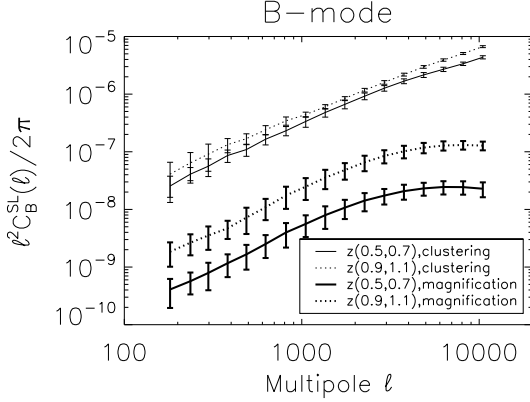


FIG. 3.— SLC induced B-mode power spectrum in the standard estimator, for the case of intrinsic source clustering (thin lines) and cosmic magnification (thick lines). $b_g = 1$ and $g = 1$ are adopted. Solid and dotted lines are for photo- z bins (0.5, 0.7) and (0.9, 1.1), respectively. The error bars are the rms dispersion among 20 realizations. The B-mode is robustly identified in all cases.

The parity asymmetric B-mode convergence κ_B could be constructed as

$$\kappa_B(\vec{\ell}) = \hat{\gamma}_1(\vec{\ell}) \sin 2\varphi_{\vec{\ell}} - \hat{\gamma}_2(\vec{\ell}) \cos 2\varphi_{\vec{\ell}}. \quad (11)$$

Then we could obtain E/B-mode power spectrum $C_E(\ell) = \langle \kappa_E(\vec{\ell}) \kappa_E^*(\vec{\ell}) \rangle$ and $C_B(\ell) = \langle \kappa_B(\vec{\ell}) \kappa_B^*(\vec{\ell}) \rangle$.

2.4. Different estimator, different SLC

The impact of SLC effect on these two estimators could be figured out in extreme cases.

For the standard estimator Eq. 7, if we have accurate redshift measurement and infinitesimal redshift bin size, the correlation between intrinsic source clustering and lens will be eliminated, $\langle \delta_g \delta'_g \gamma_i \gamma'_j \rangle \rightarrow \langle \delta_g \delta'_g \rangle \langle \gamma_i \gamma'_j \rangle$. Thus in this case the normalization will perfectly cancel the SLC induced by the intrinsic source clustering, $\hat{\xi}_{ij} \rightarrow \xi_{ij} \equiv \langle \gamma_i \gamma'_j \rangle$. However, in the context of lensing tomography with photo- z measurement, there exists significant correlation between the source and lens (Fig. 1). The investigation in this paper will quantitatively give us a conclusion about how large the SLC effect is and its dependence on redshift, scale and galaxy bias. For the cosmic magnification, $\delta^{\text{obs}} = g\kappa$ always perfectly correlates with the lensing signal. Thus inevitably the standard estimator will suffer from the cosmic magnification. Adopting analytical analysis, the amplitude is expected to be proportional to $g \langle \kappa \gamma_i \gamma'_j \rangle / \langle \gamma_i \gamma'_j \rangle$.

For the pixel-based estimator Eq. 9, in the limit of constant $g\kappa$ across the photo- z bin, $\int (1 + g\kappa) \gamma_i dz \rightarrow (1 + g\kappa) \int \gamma_i dz$. Thus the normalization for each pixel will cancel the cosmic magnification induced SLC, leading to $\hat{\gamma}_i \rightarrow \gamma_i$ and $\hat{\xi}_{ij} \rightarrow \xi_{ij}$. The following investigation will tell us the SLC induced by the cosmic magnification is indeed negligible. However, the intrinsic source clustering is not a smooth function of redshift. Even worse, for low redshift the amplitude is not weak enough to make analytical analysis. Simulation is of great help to investigate this problem.

2.5. Quantification

Through N-body simulation, we can construct 2D maps of source and lens at various redshifts to robustly quantify the SLC effect. We adopt the Born approximation for lensing map construction. The SLC effect persists under the Born approximation, since at least it keeps the leading order clustering between sources and lenses. Hence it is sufficient to adopt the Born approximation to study the SLC effect. This allows us to construct lensing maps by stacking randomly rotated and shifted simulation boxes. For details of map construction, we refer the readers to the Appendix. With these simulated maps we are able to calculate the SLC straightforwardly.

We consider two typical photo- z bins (0.5, 0.7) and (0.9, 1.1). This allows us to investigate the dependence of SLC on source redshift. We investigate two measures of SLC. (1) One is the B-mode power spectrum $C_B^{SL}(\ell)$. Without SLC, the simulated cosmic shear has vanishing B-mode. So $C_B^{SL}(\ell)$ provides a useful measure of SLC. (2) The other is the ratio of the E-mode power spectra in the presence and in the absence of SLC effect,

$$R(\ell) \equiv \frac{C_E^{SL}(\ell)}{C_E(\ell)}. \quad (12)$$

We measure it for the two auto-power spectra and one cross-power spectrum between the two redshift bins.

We are also interested in the dependences of SLC on the galaxy bias b_g and magnification prefactor g . Understanding these dependences helps calibrate the SLC effect. We choose $b_g = 0.5, 1, 1.5, 2$ and $g = -1, 1, 1.5, 2$ to study these dependences. We just substitute different b_g and g values in the construction of $\delta^{\text{obs}}(\hat{n}, z)$. To avoid unrealistic $\delta^{\text{obs}}(\hat{n}, z) < -1$, which could happen if $b_g > 1$ or $g \gg 1$, we simply set $\delta^{\text{obs}}(\hat{n}, z) = -1$ where it happens.

3. SLC WITH THE STANDARD ESTIMATOR

This section presents our results for the impact of SLC on lensing power spectrum measured with the standard estimator.

3.1. Intrinsic Source Clustering

We take $\delta^{\text{obs}} = b_g \delta_m$ in Eq. 7 to quantify SLC effect due to the intrinsic source clustering. We adopt $b_g = 1$ first.

3.1.1. B-mode power spectrum

The B-mode power spectrum is presented in Fig. 3, which is about 3 orders of magnitude lower than the E-mode. Despite its small amplitude, the measurement of B-mode is robust, since its amplitude is 5 orders of magnitude larger than the case neglecting SLC effect, i.e. setting $\delta^{\text{obs}} = 0$ (which is not presented here). The B-mode amplitude is larger for higher photo- z bin (0.9, 1.1). But this does not mean that the SLC effect is larger. Direct comparison of B-mode at the two redshifts is less meaningful, since the E-mode signal is also larger for higher redshift.

3.1.2. E-mode power spectrum

The impact of SLC on the E-mode auto- and cross-power spectrum, quantified by the ratio R (Eq. 12), is

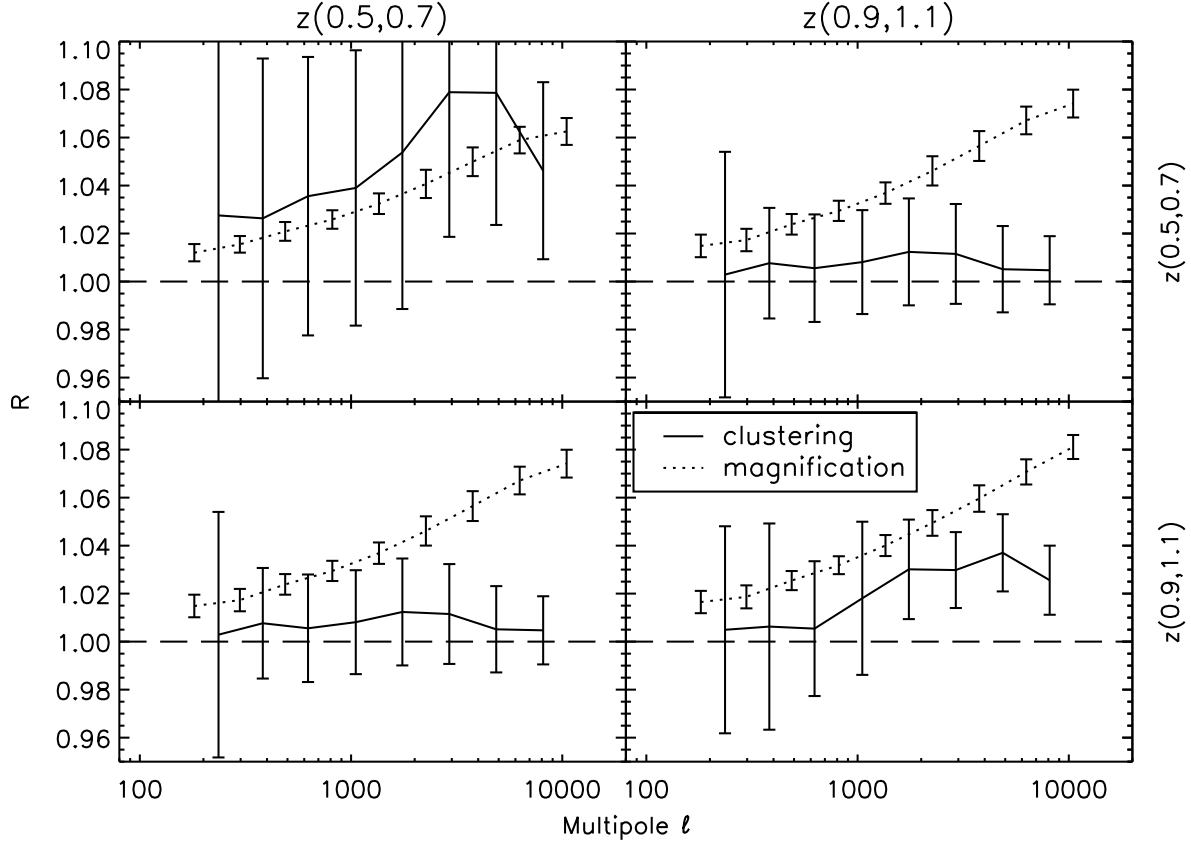


FIG. 4.— The impact of SLC on the lensing auto- and cross-power spectrum measured by the standard estimator. We plot the ratio of the power spectra $R = C_E^{\text{SL}}(\ell)/C_E(\ell)$, for $b_g = 1$ and $g = 1$, and for photo- z bins (0.5, 0.7) and (0.9, 1.1). 512^3 uniform grid is adopted in the calculation. The error bars are estimated from 20 realizations. SLC can bias the lensing E-mode power spectrum measurement by 1%-8% and the exact value depends on the galaxy bias (b_g) and the magnification pre-factor (g).

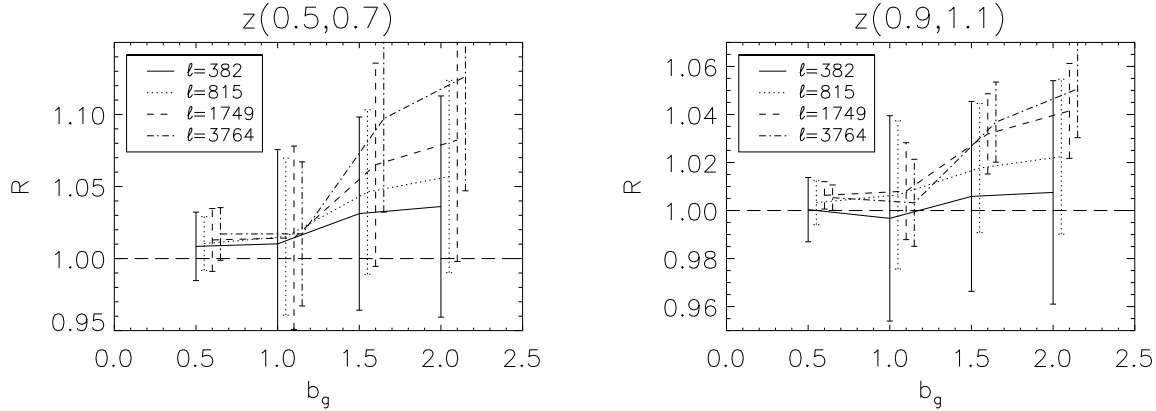


FIG. 5.— The dependence of $R = C_E^{\text{SL}}(\ell)/C_E(\ell)$ on b_g for standard estimator. The data points have $b_g = 0.5, 1, 1.5, 2$ respectively. For clarity, the results for different ℓ 's are presented with arbitrary horizontal shifts. The dependence on galaxy bias is nonlinear.

shown in Fig. 4. Although the measurement on R has large statistical uncertainty, we find $R > 1$. For $b_g = 1$, SLC amplifies the lensing E-mode power spectrum by 1-8% at $100 \lesssim \ell \lesssim 10^4$ for the photo- z bin (0.5, 0.7). The impact becomes weaker at the higher photo- z bin (0.9, 1.1). But its amplitude is still of the order 1% and hence non-negligible for precision weak lensing cosmology.

This overestimation of the E-mode lensing power spec-

trum by the standard estimator is caused by the positive cross correlation coefficient between the lensing signal and the galaxy intrinsic clustering (See Fig. 1 and Eq. 2). Although in Valageas (2014) negative correlation functions are found in some high-order correlation terms at large scales, it is not in contradiction with our result of positive cross correlation coefficient on all scales. One difference between the two is that our approach includes all the high-order corrections. The other difference is

that we describe the SLC in terms of power spectrum ratio instead of correlation function ratio. In general cases, correlation functions become negative at large scales due to the normalization. We prefer to use power spectrum since the errors in modes are independent at large scales or under linear evolution. However the description and explanation using correlation functions is more straightforward and in principle they are consistent. From Eq. 7,

$$\hat{\xi}_{ij} - \xi_{ij} = \frac{\langle (\delta_g + \delta'_g) \gamma_i \gamma'_j \rangle + \langle \delta_g \gamma'_j \rangle \langle \delta'_g \gamma_i \rangle + \langle \delta_g \gamma_i \delta'_g \gamma'_j \rangle_c}{1 + \langle \delta_g \delta'_g \rangle}. \quad (13)$$

Since the intrinsic galaxy distribution is positively correlated with the lensing signal, the standard estimator overestimates the lensing power spectrum and we expect $R - 1 > 0$.

In contrast, the impact of SLC on the lensing cross-spectrum is much weaker and the measured $R - 1$ is consistent with zero, within the error bars. For this case, we have

$$\hat{\xi}_{ij} - \xi_{ij} = \langle (\delta_g + \delta'_g) \gamma_i \gamma'_j \rangle. \quad (14)$$

Hence we expect a weaker SLC effect. However, the above result shows that the SLC effect on cross-power spectrum is non-zero, although we lack the statistical accuracy to measure it.

We find that the standard estimator results in large cosmic variance in the power spectrum measurement (Fig. 4). For example, statistical fluctuation in R is $\sim 5\%$ for the photo- z bin (0.5, 0.7) over the angular scale $100 \lesssim \ell \lesssim 10^4$. In particular, the cosmic variance does not decrease toward smaller angular scales, as we would expect. This is in sharp contrast with statistical fluctuation in the true E-mode lensing power spectrum or the angular galaxy power spectrum (Fig. 6).

We believe that this large cosmic variance is the result of modulation of the denominator ($1 + \xi_{\delta_g}$) in the standard estimator (Eq. 7). Since the correlation between the lensing signal and the galaxy field is not strong, statistical fluctuation in the galaxy field ($\delta \xi_{\delta_g}$) is only partly eliminated in the standard estimator (Eq. 7). So it contributes to fluctuation in the measured lensing correlation function/power spectrum. Since the galaxy clustering is much stronger than the lensing signal ($C_{mm}/C_{\kappa\kappa} \sim 10^3$, Fig. 6), statistical fluctuation in the denominator can cause much larger (fractional) fluctuation in the measured lensing correlation function/power spectrum. This also explains the reduced error bars towards higher redshift, for the increasing magnitude of lensing signal and decreasing magnitude of ξ_{δ_g} .

3.1.3. Dependence on b_g

We neglect the evolution of galaxy bias across the redshift bin we consider. The results for $b_g = 0.5, 1, 1.5, 2.0$ we arbitrarily choose are shown in Fig. 5. The dependence on b_g is clearly nonlinear. This more complicated behavior is already implied by Eq. 13. From it, we have

$$R - 1 = \frac{b_g f_1(\ell) + b_g^2 f_2(\ell)}{1 + b_g^2 f_3(\ell)} \simeq b_g f_1 + b_g^2 f_2 - b_g^3 f_1 f_3 + \dots, \quad (15)$$

in which f_1, f_2, f_3 are some functions of the underlying matter density δ_m and the lensing signal γ . Since the density fluctuation is of the order unity (Fig. 6), f_2 is comparable to f_1 , leading to deviation from the linear dependence.

In principle we can fit the above results to obtain a fitting formula for the R - b_g relation. Such relation is useful to calibrate SLC in the standard estimator. b_g (up to a normalization) can be directly measured from the lensing survey. So by splitting source galaxies into flux bins (with different b_g), we can measure C_E^{SL} - b_g relation and extrapolate to obtain C_E in the limit of $b_g = 0$. Unfortunately our simulation does not have sufficient independent realizations to beat down statistical fluctuations in R (Fig. 5), so we postpone more detailed investigation of R - b_g relation into future works.

More careful analysis should be carried out against mock galaxy catalogue with galaxies of various types. Nevertheless, results here have robustly shown that SLC is non-negligible in the lensing correlation function/power spectrum measured through the standard estimator.

3.2. Cosmic Magnification

We take $\delta^{\text{obs}} = g\kappa$ in Eq. 7 to quantify the SLC effect due to the cosmic magnification. In the analysis, we neglect the change of g across the redshift bin we consider. Unless for very bright galaxies in the exponential tail, this approximation is sufficiently accurate. Firstly we assume $g = 1$. We then try other values of g from -1 to 2 .

3.2.1. B-mode power spectrum

The B-mode caused by the cosmic magnification induced SLC is robustly identified (Fig. 3). It is 2 orders of magnitude lower than the one due to the intrinsic source clustering and 5 orders of magnitude lower than the lensing E-mode. Hence it is too weak to detect in lensing surveys. However, this does not mean its impact on the E-mode lensing power spectrum is negligible. In contrast, its impact on the E-mode power spectrum is 4 orders of magnitude larger than the amplitude of B-mode itself. As shown in Fig. 4, the SLC caused by this cosmic magnification affects the lensing E-mode power spectrum by a few percent. This is an example showing the danger of using B-mode as a diagnostic of lensing systematic errors.

3.2.2. E-mode power spectrum

SLC induced by the cosmic magnification has significant impact on the lensing E-mode power spectrum (Fig. 4). For example, at $\ell = 1000$ of particular interest in weak lensing cosmology, it enhances the lensing power spectrum by 3% for photo- z bin (0.5, 0.7) and 4% for photo- z bin (0.9, 1.1). The SLC effect on the cross-spectrum falls in between. The SLC effect also increases with ℓ , from 1% at $\ell \simeq 200$ to 6% at $\ell \simeq 10^4$, for the photo- z bin (0.5, 0.7). These behaviors can be roughly understood as follows. From Eq. 7, we have (also refer

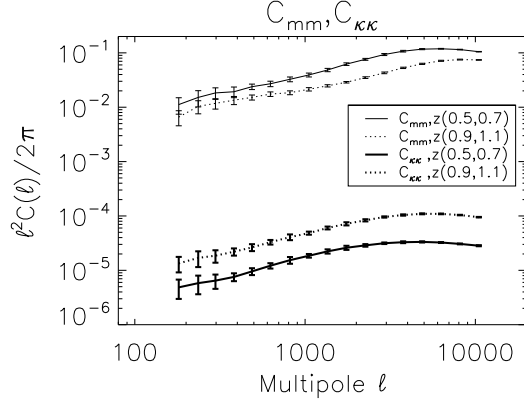


FIG. 6.— The lensing power spectrum C_{KK} and the galaxy angular power spectrum with $b_g = 1$ (C_{mm}) for photo- z bins (0.5, 0.7) and (0.9, 1.1). Large fluctuations in the galaxy distribution enhance statistical fluctuations in the lensing power spectrum measured by the standard estimator.

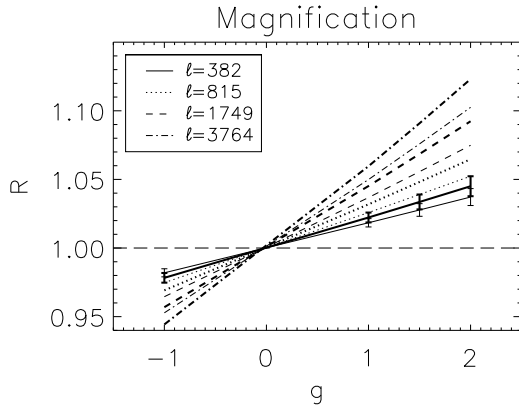


FIG. 7.— The dependence of $R = C_E^{\text{SL}}(\ell)/C_E(\ell)$ on g for standard estimator. Results are for photo- z bins (0.5, 0.7) (thin lines) and (0.9, 1.1) (thick lines). The data points have $g = -1, 1, 1.5, 2$, respectively. For clarity, we only plot the error bars for $\ell = 382$, which are the rms dispersion among 20 realizations. The dependence on g is perfectly linear.

to Schmidt et al. (2009))

$$\hat{\xi}_{ij} - \xi_{ij} = \frac{2g\langle\kappa\gamma_i\gamma_j'\rangle + g^2\langle\kappa\gamma_j'\rangle\langle\kappa'\gamma_i\rangle + g^2\langle\kappa\gamma_i\kappa'\gamma_j'\rangle_c}{1 + g^2\xi_{KK}} \simeq 2g\langle\kappa\gamma_i\gamma_j'\rangle. \quad (16)$$

The last expression has adopted the approximation $|\kappa| \ll 1$. The leading order correction $\langle\kappa\gamma\gamma'\rangle$ grows faster than $\langle\kappa\kappa\rangle$ towards small scale and high redshift, so $R - 1$ increases with both source redshift and ℓ (Fig. 4).

In contrast to the case of the intrinsic source clustering, R among realizations show weaker fluctuations (Fig. 4). The reason is that statistical fluctuations in the denominator and the numerator of the standard estimator are strongly correlated and hence are largely cancelled out.

3.2.3. Dependence on g

Eq. 16 predicts, for the auto-power spectrum,

$$R(\ell) - 1 = c(\ell)g. \quad (17)$$

Here $c(\ell)$ is determined by the ratio of lensing bispectrum and power spectrum, so it only depends on ℓ . This relation is confirmed to high accuracy in Fig. 7, where results for arbitrarily selected $g = -1, 1, 1.5, 2$ are presented. This linear relation holds for the two redshift bins and angular scales investigated ($\ell = 382, 815, 1749, 3764$). Notice that g could be zero or negative, leading to no correlation or anti-correlation between the source and lens.

For the cross correlation, we can derive a similar relation,

$$R(\ell) - 1 = c_f(\ell)g_f + c_b(\ell)g_b. \quad (18)$$

Here, g_f and g_b are the g prefactors of foreground and background galaxies. Again, $c_f(\ell)$ and $c_b(\ell)$ are determined by the ratio of lensing bispectrum and power spectrum for foreground and background, respectively. Note that g is also an observable in lensing survey. Thus if we further assign the source galaxies into different g -bins, according to the perfect scaling we could calibrate the SLC effect out. Furthermore, this calibration allow us to measure 3rd-order statistics ($\langle\gamma\gamma'\kappa'\rangle$ and $\langle\gamma\kappa\gamma'\rangle$) by comparing the power suffering SLC effect with the one calibrated.

3.3. Summary

From the results above, we summarize that the standard estimator suffers SLC effect induced by both the intrinsic source clustering and the cosmic magnification. Both of them cause $\mathcal{O}(1\%)$ - $\mathcal{O}(10\%)$ overestimation in lensing power spectrum at angular scale and redshift of interest. The standard estimator also results in large cosmic variance in the power spectrum measurement. Such systematic error is significant for lensing cosmology. Fortunately, SLC induced by the cosmic magnification present a perfect linear dependence on observable g . So it is very promising to self-calibrate it using this linear relation. SLC induced by the intrinsic source clustering shows nonlinear dependence on b_g . However, in principle, through simulation we could obtain a useful fitting formula and self-calibrate it.

4. SLC WITH THE PIXEL-BASED ESTIMATOR

This section presents our results on the impact of SLC on lensing power spectrum measured with the pixel-based estimator. This estimator first obtains the averaged cosmic shear on each pixel of the sky and then uses this map to measure lensing statistics.

4.1. Intrinsic Source Clustering

We take $\delta_g^{\text{obs}} = \delta_g$ in Eq. 9 to quantify the SLC effect due to the intrinsic source clustering, and look at $b_g = 1$ first. In general, all the results in this section depend on the pixel size. We present results with pixel size $0.7'$, $1.4'$ and $2.8'$ to show this dependence. But for clarity, we only plot error bars for the $2.8'$ pixel size case.

4.1.1. B-mode power spectrum

The B-mode power spectrum is presented in the left panel of Fig. 8. A non-zero B-mode is detected at high significance. Furthermore, it is orders of magnitude higher than the case without SLC. Hence the B-mode caused by the intrinsic source clustering induced SLC is robustly identified. It is slightly higher for lower photo- z

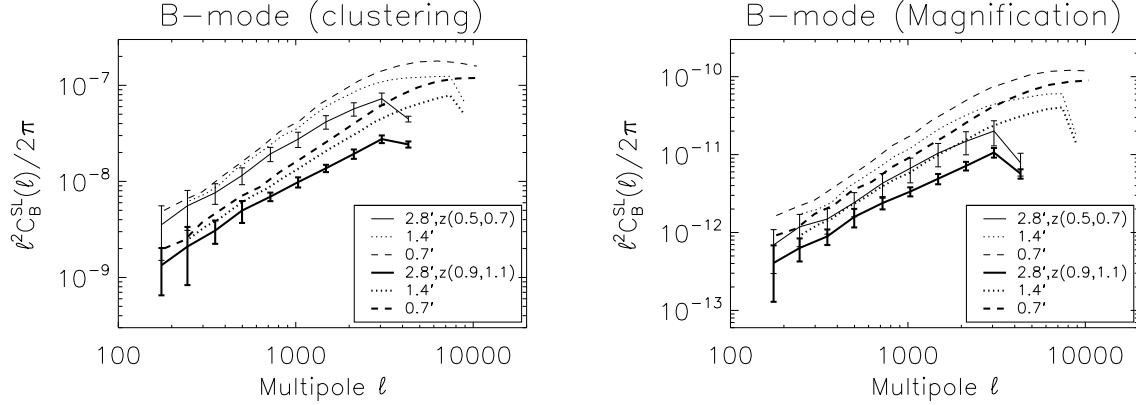


FIG. 8.— The intrinsic source clustering (left panel) and cosmic magnification (right panel) induced B-mode power spectrum measured by the pixel-based estimator (with $b_g = 1$ and $g = 1$), for photo- z bins (0.5, 0.7) (thin lines) and (0.9, 1.1) (thick lines). 3 pixel sizes, 2.8', 1.4' and 0.7', are adopted. For clarity, we only plot the error bars for the pixel size of 2.8'. The B-mode is robustly identified in all cases and the dependence on pixel size also shows up.

bin (0.5, 0.7), which is consistent with the E-mode result below. This should be due to stronger intrinsic clustering at lower redshift.

We also find smaller SLC effect for larger pixel size. Larger pixel suppresses the intrinsic clustering, leading to smaller SLC.

4.1.2. E-mode power spectrum

The impact of SLC on the lensing power spectrum is shown in Fig. 9. An immediate finding is that it suppresses the E-mode power spectrum estimation. Like the explanation for reduced skewness in Hamana et al. (2002), this behavior could be understood by considering two patterns. One pattern is that there is a source over-density near the close-side of the photo- z bin. Another is that there is an under-density near the close-side. Averaged over this photo- z bin, the lensing signal is larger in the former pattern. However, the source over-density close to us lowers the effective distance of the sources, which dilutes the lensing signal. While the under-density close to us increases the effective distance, leading to increasing of the lensing signal. This opposite direction of the SLC effect leading to the suppression of 2nd-order statistics. At $\ell \sim 1000$ of particular interest in weak lensing cosmology, this underestimation reaches 3% for the photo- z bin (0.5, 0.7) and 1% for the photo- z bin (0.9, 1.1). It increases towards small angular scale, where the intrinsic clustering is larger. This underestimation depends on the pixel size, except at scales much larger than the pixel size (e.g. the degree scale around $\ell = 200$).

A surprising result is that the cross-spectrum between the two photo- z bins is suppressed more than the auto-power spectrum of each bin. We argue that the source clustering of the two redshift bins biases the two lensing fields incoherently. Thus it reduces the coherence between the lensing signal at two redshifts and leads to larger suppression for cross-spectrum. This result is somewhat consistent with the result in Valageas (2014), which found that SLC is important when cross-correlating low and high redshift bin.

4.1.3. Dependence on b_g

The dependence of the detected underestimation on b_g is shown in Fig. 10. We find pretty good linearity for the higher photo- z bin (0.9, 1.1), and reasonably good for the lower photo- z bin (0.5, 0.7). Since our bias model is very simplified, further study against mock catalogue is required to robustly quantify R - b_g relation.

The detected 1% level bias in the measured lensing power spectrum is significant for precision lensing cosmology. Further analysis, including analysis against mock galaxy catalogue and investigations on PDF and peak statistics (Liu et al. 2013), should be carried out to fully understand the impact of SLC on weak lensing statistics based on the pixel-based estimator.

4.2. Cosmic Magnification

For the cosmic magnification induced SLC, we find that pixel-based estimator suppresses SLC to negligible level, both for the lensing B-mode (right panel of Fig. 8) and the E-mode (Fig. 9). This is valid for all the redshifts, pixel sizes and g investigated. The detected B-mode has a rms $\sim 10^{-5}$, which is orders of magnitude smaller than statistical fluctuations in cosmic shear measurement of full-sky survey. SLC affects the E-mode power spectrum by $\sim 0.1\%$ at $\ell \sim 1000$. This bias is again significantly smaller than the statistical accuracy of any realistic lensing surveys.

Why does the pixel-based estimator work so well? We argue that it is due to the fact that κ varies slowly across the photo- z bin, for each line of sight. In the limit that it can be well approximated as a constant along each line of sight, the weighting $(1 + g\kappa)$ in the numerator and denominator cancel out. So the averaged γ is area averaged, exactly what we want.

4.3. Summary

From the results above, we can conclude that the pixel-based estimator is essentially free of SLC induced by the cosmic magnification. So the SLC effect only arises from the intrinsic source clustering. It causes 1-10% underestimation of the lensing power spectrum at angular scale and redshift of interest. Such systematic error is significant for lensing cosmology. Fortunately we find that the induced SLC has a reasonably good linear dependence

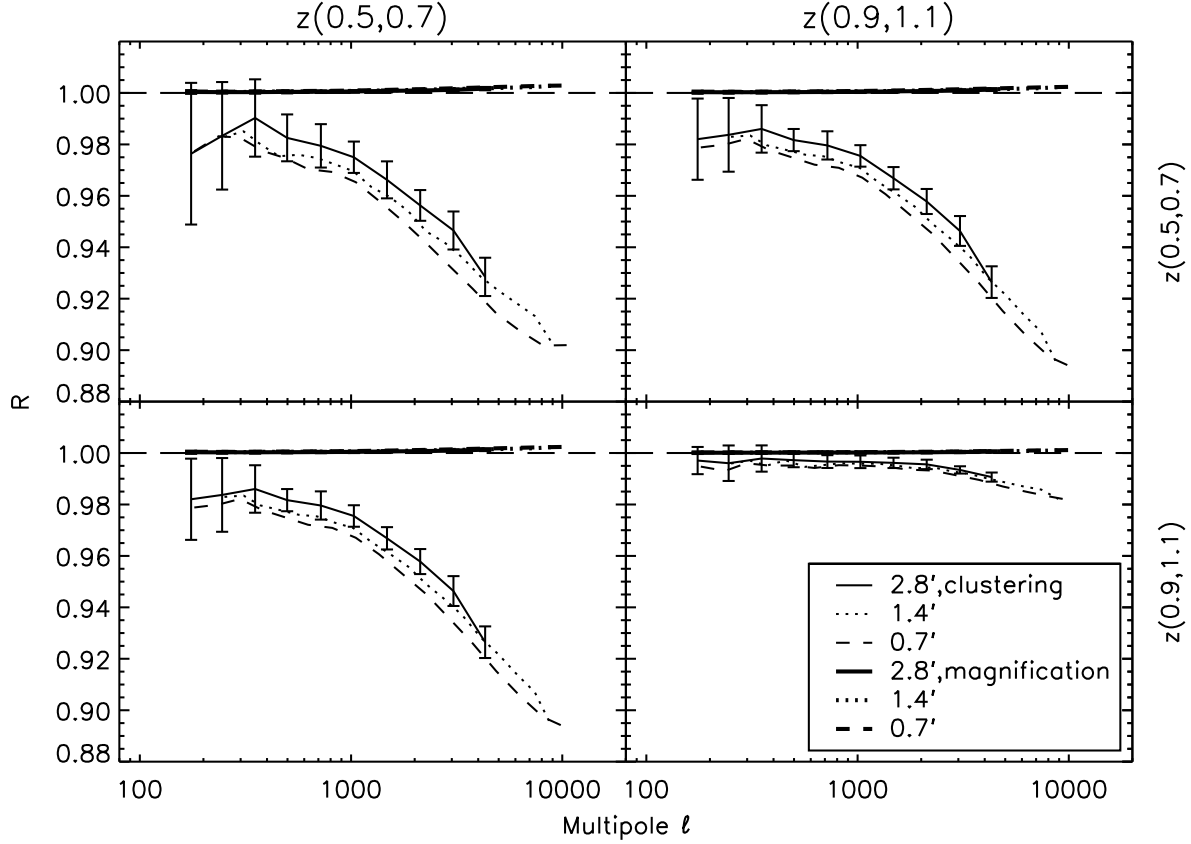


FIG. 9.— The impact of SLC on the lensing power spectrum measured by the pixel-based estimator. We plot the ratio $R = C_E^{\text{SL}}(\ell)/C_E(\ell)$, for different source redshift, different pixel size and different source of SLC. The pixel-based estimator overcorrects the SLC induced by the intrinsic source clustering, causing underestimation of the lensing power spectrum by $\sim 1\%$ at $\ell = 1000$ and $z_s \sim 1$. In contrast, it almost perfectly corrects the SLC induced by the cosmic magnification, leading to negligible bias in the measured lensing power spectrum.

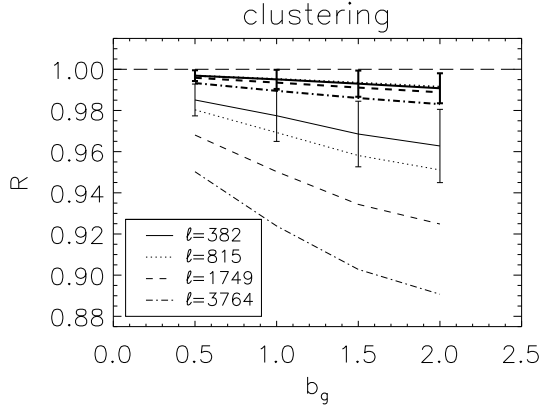


FIG. 10.— The dependence of $R = C_E^{\text{SL}}(\ell)/C_E(\ell)$ on the galaxy bias, for the pixel-based estimator. Results are for photo- z bins (0.5,0.7) (thin lines) and (0.9,1.1) (thick lines). For clarity, we only plot the errors for $\ell = 382$. The dependence on galaxy bias shows good linearity.

on the galaxy bias. So it is promising to self-calibrate the SLC effect using this linear relation.

5. CONCLUSION AND DISCUSSION

We use N-body simulation to evaluate the SLC effect in the context of weak lensing tomography with realistic photo- z errors. We quantify the effect for two kinds of

estimator, the standard estimator and the pixel-based estimator, and for two sources of the SLC effect, the intrinsic source clustering and the cosmic magnification. The statistics investigated include B-mode power spectrum, the ratio of E-mode power spectra, and the dependence on galaxy bias or magnification prefactor.

We found that in all cases, B-mode is clearly produced by the SLC effect. But the amplitude of the produced B-mode is at least 3 orders of magnitude lower than the E-mode. Thus these B-modes are not expected to be detected in near future lensing survey.

For the standard estimator, the SLC effect induced by both the intrinsic source clustering and the cosmic magnification can bias the lensing power spectrum by $\mathcal{O}(1\%)$ - $\mathcal{O}(10\%)$ at the scale and redshift of interest. Furthermore, the standard estimator brings large cosmic variance into the power spectrum measurement. But the cross power spectrum suffers much less SLC effect induced by the intrinsic source clustering. These two sources of SLC together make the situation more complicated. Fortunately, the SLC effect shows perfect linear dependence on the observable g , which comes free from the lensing survey. Thus the self-calibration is very promising. Large sky coverage will beat down the fluctuations in the SLC effect induced by the intrinsic source clustering. When this uncertainty is well under control, in principle, we could find a fitting formula for the dependence on galaxy bias and utilize it to the observation

to self-calibrate the SLC effect induced by the intrinsic source clustering.

For the pixel-based estimator, we found negligible cosmic magnification induced SLC effect. However, the intrinsic source clustering induced SLC suppresses the power spectrum measurement by $\mathcal{O}(1\%)$ - $\mathcal{O}(10\%)$. Fortunately, the dependence of SLC effect on galaxy bias shows good linearity. This linear scaling for low bias galaxies and for high redshift is also useful to self-calibrate the SLC effect.

From the results in this work, the pixel-based estimator has negligible SLC effect from the cosmic magnification. The intrinsic source clustering induced SLC effect shows good linear dependence on galaxy bias. Thus it is easy to deal with SLC effect by self-calibration. However, the standard estimator suffers severe SLC effect from both the two sources and large cosmic variance induced by the intrinsic source clustering. Although the dependence on g is perfectly linear, we need further works to deal with the SLC effect induced by the intrinsic source clustering.

For the standard estimator, the B-mode produced by intrinsic source clustering is consistent with the result in Schneider et al. (2002), in which they analytically estimated the amplitude. We caution that lensing tomography indeed could suppress SLC effect induced by intrinsic source clustering, but not to a negligible level. The large SLC effect induced by cosmic magnification is consistent with the result in Schmidt et al. (2009), in which they focused on lensing bias and analytically calculated the correction term from bispectrum. As pointed out in the literatures, the effect from approximating reduced shear as cosmic shear shares the same form with the cosmic magnification ($g = 1$). Our result is also consistent with the result for reduced shear in Dodelson et al. (2006). Thus our work here also confirms the result for reduced shear through simulation.

The SLC effect is a severe systematic error in weak lensing cosmology. We need further investigations to deal with it. The bias in cosmological parameters is one important focus. The goodness of the above self-

calibration method is also of great importance. Numerical results presented in this paper are limited by the finite box size and moderate resolution and limited realization of the analyzed N-body simulation. They should be rechecked and improved by larger simulations with higher resolution and many more realizations. Furthermore, we need more realistic lensing mock catalogue, with various types of galaxies, various photometric redshift distributions and bin schemes, to test these scaling relations and methods.

We emphasize that the two estimators are not redundant. In contrast, they are complementary to each other and provide a valuable cross-check on the lensing measurement and the SLC effect. (1) The standard estimator is convenient for direct measurement of 2-point statistics from lensing survey. (2) The pixel-based estimator is of great importance for map-making and higher-order statistics such as bispectrum and 1-point PDF. (3) Given that the underlying lensing signal is the same and given that the two estimators suffer differently from the SLC effect, with different dependence on galaxy bias and magnification prefactor, it is interesting to compare the two independent lensing measurements. Due to the negligible SLC induced by the cosmic magnification and reasonably good R - b_g relation, it seems easier to get unbiased lensing signal from the pixel-based estimator. Combining this unbiased lensing signal with the one derived from the standard estimator, it is possible to identify and isolate the SLC effect in observation.

ACKNOWLEDGMENT

This work was supported by the national science foundation of China (Grant No. 11025316, 11121062, 11033006, 11320101002, 1087302711233005, 11473053, U1331201). The work is also supported by the "Strategic Priority Research Program the Emergence of Cosmological Structures" of the Chinese Academy of Sciences, Grant No. XDB09010400. This work made use of the High Performance Computing Resource in the Core Facility for Advanced Research Computing at Shanghai Astronomical Observatory.

APPENDIX

SIMULATION

Our N-body simulation was run using the Gadget-2 code (Springel 2005) adopting the standard Λ CDM cosmology, with $\Omega_m = 0.266$, $\Omega_\Lambda = 1 - \Omega_m$, $\sigma_8 = 0.801$, $h = 0.71$ and $n_s = 0.963$. It is performed with 512^3 particles in the $300h^{-1}\text{Mpc}$ box. The simulation details can be found in Cui et al. (2010). For the purpose of lensing study, the output redshifts z_i are specified such that any two adjacent snapshots are separated by the box size $L = 300h^{-1}\text{Mpc}$ in comoving distance, i.e. $D(z_i) = 300i - 150h^{-1}\text{Mpc}$ ($i = 1, 2, 3, \dots$). For a source redshift $z_s \sim 1$, we need to stack 10 snapshots to construct one lensing map. Since each snapshot is obtained from the same initial conditions, to avoid artificial correlation, we randomly shift and rotate the boxes utilizing the periodical boundary condition. All quantities involved in SLC effect (matter overdensity, convergence, cosmic shear) are constructed as follows.

- (1) We stack 10 randomly shifted and rotated boxes to comoving distance $3000h^{-1}\text{Mpc}$. 20 light-cone realizations are made with sky coverage of $6.03^\circ \times 6.03^\circ$ each.
- (2) We cut the light-cones into density slices $\delta_{m,i}$ ($i = 1, \dots, 140$) with width $\Delta z = 0.01$, from $z = 0$ to $z = 1.4$, adopting NGP mass-assignment.
- (3) Adopting Born approximation, we construct κ_i slices also with $\Delta z_s = 0.01$, according to

$$\kappa(\hat{n}, z_s) = \int_0^{\tilde{\chi}(z_s)} \delta_m(\hat{n}, z) W(z, z_s) d\tilde{\chi} \quad (\text{A1})$$

and the corresponding discrete form

$$\kappa_i(\hat{n}) = \sum_{j=1}^{i-1} \delta_{m,j}(\hat{n}) W_{ji} \Delta z. \quad (\text{A2})$$

Here, δ_m is the matter overdensity. $\chi \equiv \chi(z)$ is the comoving angular diameter distance to the lens redshift z . We conveniently express χ in units of the Hubble radius, $\tilde{\chi} \equiv \chi/(c/H_0)$, in which H_0 is the Hubble constant today. The lensing kernel $W(z, z_s)$ for a source at redshift z_s and a lens at redshift z is given by

$$W(z, z_s) = \frac{3}{2} \Omega_m (1+z) \tilde{\chi}(z) \left[1 - \frac{\chi(z)}{\chi(z_s)} \right] \quad (\text{A3})$$

when $z \leq z_s$ and zero otherwise. The corresponding discrete form is

$$W_{ji} = \frac{3}{2} \Omega_m (1+z_j) \tilde{\chi}_j \left[1 - \frac{\chi_j}{\chi_i} \right]. \quad (\text{A4})$$

Here Ω_m is the cosmological matter density of the universe in units of the critical density. The above expression is valid for the flat cosmology we consider throughout the paper.

(4) We convert κ slices into cosmic shear slices through the relation in Fourier space

$$\gamma_1(\vec{\ell}) = \kappa(\vec{\ell}) \cos 2\varphi_{\vec{\ell}}, \quad \gamma_2(\vec{\ell}) = \kappa(\vec{\ell}) \sin 2\varphi_{\vec{\ell}}. \quad (\text{A5})$$

(5) We treat the source galaxy distribution as the number density field $\delta^{\text{obs}}(\hat{n}, z)$. For the investigation on the intrinsic source clustering, we adopt a simple bias model $\delta^{\text{obs}}(\hat{n}, z) = b_g \delta_m(\hat{n}, z)$. While for the cosmic magnification, only leading term is kept, i.e. $\delta^{\text{obs}}(\hat{n}, z) = g \kappa(\hat{n}, z)$. For general study we direct adopt $b_g = 1$ and $g = 1$. For the dependence study on b_g and g , we just multiply several typical values to construct $\delta^{\text{obs}}(\hat{n}, z)$ for each cases. We choose $b_g = 0.5, 1, 1.5, 2.0$ and $g = -1, 1, 1.5, 2$. To avoid unrealistic $\delta^{\text{obs}}(\hat{n}, z) < -1$, which could happen if $b_g > 1$ or $g \gg 1$, we simply set $\delta^{\text{obs}}(\hat{n}, z) = -1$ where it happens. We then integrate over the corresponding source redshift distribution to obtain the projected galaxy number overdensity and lensing signal.

REFERENCES

- Bartelmann, M. 2010, CQGra, 27, 233001
 Bartelmann, M., & Schneider, P. 2001, PhR, 340, 291
 Becker, M. R. 2013, MNRAS, 435, 115
 Bernardeau, F. 1998, A&A, 338, 375
 Bernstein, G., & Huterer, D. 2010, MNRAS, 401, 1399
 Bridle, S., & King, L. 2007, NJPh, 9, 444
 Bridle, S., Shawe-Taylor, J., Amara, A., et al. 2009, AnApS, 3, 6
 Chang, C., Marshall, P. J., Jernigan, J. G. et al. 2012, MNRAS, 427, 2572
 Chang, C., Kahn, S. M., Jernigan, J. G. et al. 2013, MNRAS, 428, 2695
 Cui, W., Zhang, P., & Yang, X. 2010, PhRvD, 81, 103528
 Cunha, C. E., Huterer, D., Lin, H., Busha, M. T., & Wechsler, R. H. 2012, arXiv:1207.3347
 Cunha, C. E., Huterer, D., Busha, M. T., & Wechsler, R. H. 2012, MNRAS, 423, 909
 Dodelson, S., Kolb, E. W., Matarrese, S., Riotto, A., & Zhang, P. 2005, PhRvD, 72, 103004
 Dodelson, S., Shapiro, C., & White, M. 2006, PhRvD, 73, 023009
 Dodelson, S., & Zhang, P. 2005, PhRvD, 72, 083001
 Eifler, T., Krause, E., Dodelson, S., et al. 2014, arXiv:1405.7423
 Forero-Romero, J. E., Blaizot, J., Devriendt, J., van Waerbeke, L., & Guiderdoni, B. 2007, MNRAS, 379, 1507
 Hagan, B., Ma, C.-P., Kravtsov, A.-V. 2005, ApJ, 633, 537
 Hamana, T. 2001, MNRAS, 326, 326
 Hamana, T., Colombi, S. T., Thion, A., et al. 2002, MNRAS, 330, 365
 Hamana, T., Miyazaki, S., Okura, Y., Okamura, T., & Futamase, T. 2013, PASJ, 65, 104
 Harnois-Déraps, J., van Waerbeke, L., Viola, M., & Heymans, C. 2014, arXiv:1407.4301
 Hearin, A. P., Zentner, A. R., Ma, Z., & Huterer, D. 2010, ApJ, 720, 1351
 Heymans, C., White, M., Heavens, A., Vale, C., & van Waerbeke, L. 2006, MNRAS, 371, 750
 Heymans, C., van Waerbeke, L., Bacon, D., et al. 2006, MNRAS, 368, 1323
 Heymans, C., van Waerbeke, L., Miller, L., et al. 2012, MNRAS, 427, 146
 Hilbert, S., Hartlap, J., White, S. M. D., & Schneider, P. 2009, A&A, 499, 31
 Hirata, C. M., & Seljak, U. 2004, PhRvD, 70, 063526
 Hoekstra, H. 2004, MNRAS, 347, 1337
 Hoekstra, H., & Jain, B. 2008, ARNPS, 58, 99
 Huterer, D., Takada, M., Bernstein, G., & Jain, B. 2006, MNRAS, 366, 101
 Jain, B., Jarvis, M., & Bernstein, G. 2006, JCAP, 02, 21
 Jing, Y. 2002, MNRAS, 335, L89
 Jing, Y., Zhang, P., Lin, W., Gao, L., & Springel, V. 2006, ApJ, 640, L119
 Joachimi, B., & Bridle, S. 2010, A&A, 523, 1
 Joachimi, B., & Schneider, P. 2008, A&A, 488, 829
 Kilbinger, M., Schneider, P., & Eifler, T. 2006, A&A, 457, 15
 Liu, J., Haiman, Z., Hui, L., Kratochvil, J. M., & May, M. 2013, arXiv:1310.7517
 LSST Dark Energy Science Collaboration 2012, arXiv:1211.0310
 Ma, Z., Hu, W., & Huterer, D. 2006, ApJ, 636, 21
 Mandelbaum, R., Rowe, B., Bosch, J., et al. 2014, ApJS, 212, 5
 McDonald, P., Trac, H., Contaldi, C., 2006, MNRAS, 366, 547
 Munshi, D., Valageas, P., van Waerbeke, L., & Heavens, A. 2008, PhR, 462, 67
 Okumura, T. & Jing, Y. 2009, ApJ, 694, L83
 Okumura, T., Jing, Y., & Li, C., 2009, ApJ, 694, 214
 Refregier, A. 2003, ARA&A, 41, 645
 Rudd, D. H., Zentner, A. R., & Kravtsov, A. V. 2008, ApJ, 672, 19
 Schmidt, F., Rozo, E., Dodelson, S., Hui, L., & Sheldon, E. 2009, ApJ, 702, 593
 Schneider, P., van Waerbeke, L., Jain, B., & Kruse, G. 1998, MNRAS, 296, 873
 Schneider, P., van Waerbeke, L., & Mellier, Y. 2002, A&A, 389, 729
 Semboloni, E., Hoekstra, H., & Schaye, J. 2013, MNRAS, 434, 148
 Semboloni, E., Hoekstra, H., Schaye, J., van Daalen, M. P., & McCarthy, I. G. 2011, MNRAS, 417, 2020
 Springel, V. 2005, MNRAS, 364, 1105
 Troxel, M. A., & Ishak, M. 2012, MNRAS, 419, 1804
 Troxel, M. A., & Ishak, M. 2012, MNRAS, 423, 1663
 Troxel, M. A., & Ishak, M. 2012, MNRAS, 427, 442
 van Daalen, M. P., Schaye, J., Booth, C. M., & Vecchia, C. D. 2011, MNRAS, 415, 3649
 van Daalen, M. P., Schaye, J., McCarthy, I. G., Booth, C. M., & Vecchia, C. D. 2014, MNRAS, 440, 2997
 Valageas, P. 2014, A&A, 561, 53
 van Waerbeke, L., White, M., Hoekstra, H., & Heymans, C. 2006, APh, 26, 91

- White, M., 2004, APh, 22, 211
Zentner, A. R., Rudd, D. H., & Hu, W. 2008, PhRvD, 77, 043507
Zentner, A. R., Semboloni, E., Dodelson, S., et al. 2013, PhRvD, 87, 043509
Zhan, H., & Knox, L. 2004, ApJ, 616, L75
Zhang, P. 2010, ApJ, 720, 1090
Zhang, P. 2010, MNRAS, 406, L95
Zhang, J., & Komatsu, E. 2011, MNRAS, 414, 1047
Zhang, P., Pen, U., & Bernstein, G. 2010, MNRAS, 405, 359